IEEE Access
Multidisciplinary | Rapid Review | Open Access Journal

Received 14 June 2022, accepted 20 July 2022, date of publication 25 July 2022, date of current version 28 July 2022.

Digital Object Identifier 10.1109/ACCESS.2022.3193509

RESEARCH ARTICLE

Driving Cycle Recognition Based Adaptive Equivalent Consumption Minimization Strategy for Hybrid Electric Vehicles

DONGDONG CHEN[1], TIE WANG[1,2], TIANYOU QIAO[1], TIANTIAN YANG[1], AND ZHIYONG JI[1]

[1]College of Mechanical and Vehicle Engineering, Taiyuan University of Technology, Taiyuan 030024, China
[2]Centre for Efficiency and Performance Engineering, University of Huddersfield, Queensgate, Huddersfield HD1 3DH, U.K.

Corresponding author: Tie Wang (wangtie57@163.com)

This work was supported in part by the National Natural Science Foundation of China under Grant 51805353.

ABSTRACT Hybrid electric vehicles (HEVs) are considered the most practical option for reducing emissions and fuel consumption of conventionally powered vehicles. Energy management strategies (EMSs) are the core technology of HEVs because of decreasing the cost of the system and limiting its negative effects. Equivalent consumption minimization strategy (ECMS) can achieve instantaneous optimal control and has attracted attention in recent years. In this study, an adaptive equivalent consumption minimization strategy (A-ECMS) based on driving cycle recognition is constructed for a parallel HEV. First, select the standard driving cycle and analyze its characteristic parameters. And then training learning vector quantization (LVQ) neural network-based driving cycle recognizer to achieve an average of 98% accuracy. At last, the optimal equivalent factor (EF) is selected for ECMS by recognizing the current driving cycle. It is jointly simulated and analyzed by AVL CRUISE and MATLAB/Simulink software under NEDC and CHTC-LT driving cycle. The results show that compared with the logic-based EMS, in the NEDC driving cycle the 100 km fuel consumption of A-ECMS decreases by 3.8%, and the battery state of charge (SOC) increases by 1.1%. In the CHTC-LT driving cycle, fuel economy improves by 3.6%, proving the superiority of the A-ECMS.

INDEX TERMS Hybrid electric vehicle (HEV), energy management strategy (EMS), equivalent consumption minimization strategy (ECMS), driving cycle recognition, learning vector quantization (LVQ).

I. INTRODUCTION

With the intensification of environmental pollution and shortage of oil resources, people pay more and more attention to the environmental protection and energy saving of vehicles. Today, the world is grappling with concerns about oil conservation and hazardous emissions, prompting a major shift in technology from traditional internal combustion engine (ICE)-powered automobiles to more energy-efficient automobile powertrains. Due to the limitations of battery technology, electric vehicles have the fatal defects of short-range and low energy density. Low energy density and high cost are the main challenges to developing commercially viable all-electric vehicles. With more than two power sources, HEV combines the advantages of both electric vehicles and conventional internal combustion engine vehicles.

The EMS controls the power flow of the vehicle and thus fully exploits the energy-saving and emission reduction potential of the HEV [1], [2]. According to the different control methods, the EMSs of HEVs can be divided into three categories: rule-based, optimization-based, and learning-based EMS. The optimization-based EMS control method includes global optimization, transient optimization, and model predictive control (MPC) [3]. Rule-based EMSs are widely used in real vehicles, including logic threshold strategies and fuzzy logic strategies. The logic threshold strategy mainly analyzes the opening and change rate of the accelerator pedal and brake pedal to determine the demand power of the vehicle. Then it combines the state input of the vehicle to determine the corresponding output variables so that the engine always runs in the high-efficiency zone [4]–[6].

The associate editor coordinating the review of this manuscript and approving it for publication was Bin Zhou.

The global optimization-based EMS applied the optimal control theory to dynamically allocate torque for the entire driving cycle [7]–[9]. However, the MPC-based EMS is to transform the global optimization problem in the whole driving cycle which is a local optimization problem in the prediction time domain. Through rolling optimization, researchers obtained better optimization results by continuously updating the future driving state of the vehicle in the prediction time domain [10]–[12]. The transient optimization-based EMS takes transient fuel consumption as the optimization target. It allocates the output power of different power sources to minimize the transient consumption under an unknown driving cycle [13]–[15]. Compared with rule-based EMSs, these methods usually take the instantaneous fuel consumption as the optimization target and calculate the energy allocation in real-time that mainly including the ECMS and Pontryagin's minimum principle (PMP) [16], [17]. The control strategy parameters are optimized by learning-based EMS that learns from historical data and forecast information [18], [19].

The ECMS achieves instantaneous optimality by equating electrical consumption to fuel consumption through an equivalence factor (EF). Any stored electrical energy used during the battery discharge phase is replenished at a later stage using engine fuel or through regenerative braking in an HEV [20]. The conventional ECMS considers the EF a constant value, while the adaptive EF varies with SOC values and driving cycle. Research on ECMS-based EMSs focuses on optimizing the EF. There are three main approaches to adaptive EF: SOC-based feedback, driving cycle recognition-based, and driving cycle prediction-based.

By adjusting the EF through SOC deviation feedback, the method proved to effectively control the SOC to vary within a certain range and keep the SOC stable. Wang *et al.* [21] investigated a SOC obtained by dynamic programming (DP) global optimization algorithm as a reference SOC for A-ECMS. Fan *et al*. [22] used the DP algorithm to extract the mode switching boundaries and shifting laws under three typical operating conditions and established a reference SOC by using the PI algorithm and adjusting the EF. Guan *et al.* [23] designed the SOC expectation trajectory based on the difference between the initial SOC and the minimum SOC divided by the remaining mileage and used a fuzzy controller with SOC feedback to correct the EF.

The optimal EF for the typical driving cycle is calculated offline by using the historical driving cycle information. Then the current driving cycle is identified online by the historical driving cycle information. The algorithm that analyzes the historical driving cycle is called the identification algorithm. Han *et al.* [24] used a particle swarm optimization algorithm. The real historical traffic data offline to establish the mapping table of SOC and power demand, obtained the EF of SOC optimal trajectory by SOC and recursive neural network. Zhang *et al.* [25] used the principal component analysis method to extract the characteristic parameters of the driving cycle based on cluster analysis. They identified driving conditions and automatically adjust the EF to the actual driving cycle. Guo *et al.* [26] used a hybrid particle swarm optimization genetic algorithm to optimize the relationship between driving style and EF. They analyzed the accelerator pedal opening and its change rate under different driving cycles and established a fuzzy logic recognizer to identify the driving cycle. Shi *et al.* [27] developed a method to identify driving cycle types in real-time with higher accuracy and apply a driving cycle identification model based on a support vector machine optimized by a particle swarm algorithm to ECMS.

The prediction range is generally short in predicting future driving cycles by algorithms. Another method is to use information from external devices such as GPS, intelligent transportation systems, and vehicle networks to predict driving cycles over longer distances and adjust the EF in advance. Lin *et al.* [28] established an EF model based on the energy required per unit distance. The EF correction was optimized by using the particle swarm optimization method and the future driving cycle was predicted by using an artificial neural network, and the EF estimation model was updated online. Zhang *et al.* [29] established an ECMS prediction model by predicting vehicle speed through back propagation (BP) neural network and designed dynamic adaptive EF according to the future driving cycle. Zhang *et al.* [30] proposed a chain neural network to predict the speed in different time ranges for application to ECMS. Sun *et al.* [31] constructed a neural network-based speed predictor to predict future short-term driving behavior by learning from historical data and combined it with an A-ECMS to provide temporary driving information for real-time EF.

Learning vector quantization (LVQ) is an output forward artificial neural network for training output competitive, and output layers, which is widely used in recognition, diagnosis, and optimization fields. If two or more input vectors are close to each other, the competitive layer will classify them into the same class. Compared with other pattern recognition, LVQ lattices are simple and do not require complex neural network structures, but only the distance between their competing neurons [32], [33]. However, LVQ has rarely been applied to the study of driving cycle recognition. In this study, an LVQ-based driving cycle recognition method is proposed to combine with ECMS to optimize the EF.

Taking a single-axle parallel HEV light-duty truck as the research object, the logic-based EMS and ECMS is first built. Based on the ECMS, an LVQ-based recognizer of driving cycles is designed with fuel economy as the optimization target to optimize the EF. The verification of the EMSs is carried out by joint simulation of AVL Cruise and MATLAB/Simulink under the driving cycle of the China heavy-duty commercial vehicle test cycle-truck (CHTC-LT) and the new European driving cycle (NEDC).

II. HEV MODELING

The research object of this paper is a parallel HEV of P2 configuration, as shown in Fig. 1, which consists of a diesel engine, clutch, integrated starter generator (ISG) electric motor, six-speed transmission, and battery. It can realize

TABLE 1. Main system parameters.

Parts	Parameter Name	Value
Vehicles	Overall mass / kg	2500
	Full load mass / kg	4500
	Wheelbase / mm	3300
	Tire rolling radius / mm	402.5
	Windward area / m^2	4.6
	Rolling resistance coefficient	0.015
	Wind resistance coefficient	0.7
	Main reduction ratio	4.875
Engine	Displacement / L	2.499
	Number of cylinders / pc	4
	Rated speed / (r/min)	3600
	Maximum torque / (N·m)	360
	Maximum output power / kw	105
Electric motor	Maximum power / kw	67
	Rated power / kw	50
	Maximum torque / (N·m)	400
	Rated torque / (N·m)	300
	Maximum speed / (r/min)	6000
Battery	Battery pack capacity / Ah	80
	Total battery pack voltage / V	320

electric motor (EM) drive mode, drive charging mode, hybrid drive mode, regenerative braking mode, and engine drive mode. When the vehicle demand torque is small at the start, the EM provides the power completely. When the vehicle demand torque is large, the engine is working, and the EM is in drive motor mode or generator mode according to the vehicle driving state. When the SOC is lower than the threshold value, the engine is the only power source, and the excess torque is used to drag the motor to generate electricity. When the vehicle decelerates and brakes, the size of the mechanical braking force is determined according to the current vehicle speed and SOC. The main parameters of the study model are shown in Table 1.

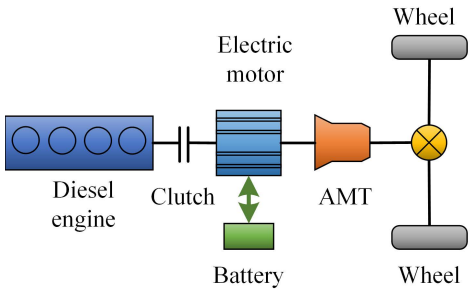

FIGURE 1. A parallel HEV with P2 configuration.

A. ENGINE MODEL

In this paper, by using experimental modeling to get the engine characteristic curve according to the bench test and established the input-output relationship. The engine universal characteristics diagram is shown in Fig. 2.

The engine output torque is calculated by (1).

$$T_e = f_{\text{torque}}(a_e, n_e) \tag{1}$$

The engine fuel consumption rate is calculated by (2).

$$m_f = f_{\text{fuel}}(T_e, n_e) \tag{2}$$

where a_e is the engine accelerator pedal opening; n_e is the engine rotational speed, r/min; T_e is the engine torque, N·m; and m_f is the engine fuel consumption rate, g/(kW·h).

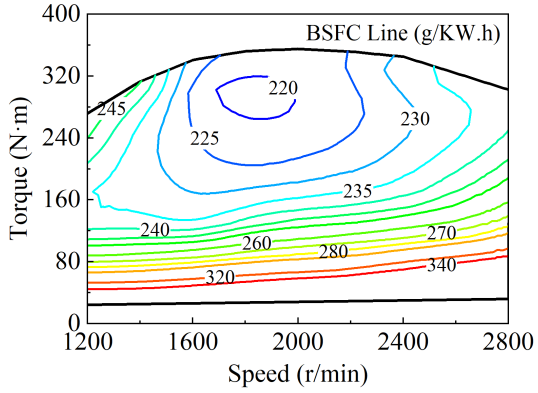

FIGURE 2. Universal characteristics curve of engine.

B. ELECTRIC MOTOR MODEL

The EM modeling method is experimental modeling, and the efficiency characteristics diagram is shown in Fig. 3.

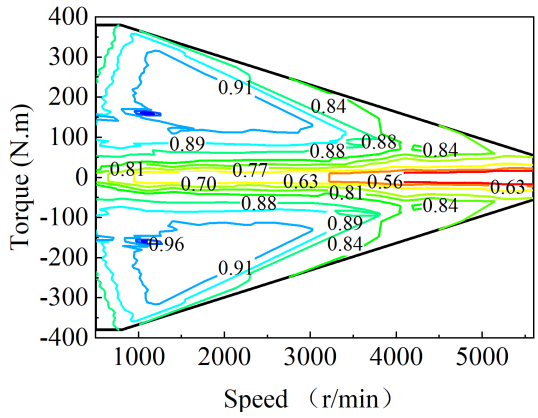

FIGURE 3. EM efficiency characteristics diagram.

The efficiency of the EM is calculated by (3).

$$\eta_m = \eta(n_m, T_m) \tag{3}$$

The power of the EM is calculated by (4).

$$P_m = \begin{cases} \frac{T_m n_m}{\eta_m}, T_m \geq 0 \\ T_m n_m \eta_m, T_m < 0 \end{cases} \tag{4}$$

where n_m is the EM rotational speed; T_m is the EM torque; η_m is the EM efficiency; P_m is the EM power.

C. BATTERY MODEL

According to the voltage drop characteristics during battery use, the battery charge and discharge efficiency curve is used to determine the relationship between battery voltage and SOC.

TABLE 2. Shift logic.

Gear	Gear ratio	Upshift speed (km/h)	Downshift speed (km/h)
1	6.14	10	10
2	3.36	18.5	18.5
3	2.11	29.5	29.5
4	1.34	46.5	46.5
5	1	62.25	62.25
6	0.7	100	100

The battery SOC is calculated by (5).

$$SOC = SOC_0 + \frac{1}{3600C}\int_{t_0}^{t} Idt \tag{5}$$

The battery current is calculated by (6).

$$I = \frac{U - \sqrt{U^2 - 4RP_b}}{2R} \tag{6}$$

where SOC_0 is the initial SOC; C is the battery capacity; U is the open-loop battery voltage; R is the battery internal resistance, and P_b is the battery power.

D. GEAR TRANSMISSION MODEL

The gear transmission is a 6-speed automatic transmission. This refers to six gears within the transmission. The transmission control module controls the automatic transmission shift process, and the specific shift control is shown in Table 2.

E. PHYSICAL MODEL

Based on the above model, an HEV simulation model was built in AVL CRUISE as shown in Fig. 4. Calibrate mechanically and electrically connect the engine, clutch, EM, and other components. The mechanical connect is used to transmit the mechanical signal, and torque output from the engine. Through the clutch, transmission, main gearbox, and differential, mechanical connect is converted into the driving force of the wheels. The electrical connections transmitted electrical signals and connect the motor, battery, and electrical accessories. The monitor module can be connected to any module's input and output signals.

F. EXPERIMENTAL VALIDATION

This paper ensures the model's credibility by comparing and verifying the fuel consumption variation curves of the bench test and simulation results. The single-axis parallel hybrid power system test bench is mainly composed of a diesel engine, hydraulic clutch, ISG EM, electric dynamometer, analog power supply, water cooling system, and control system as shown in Fig. 5.

Fig. 6 shows the test condition points selected in the NEDC, it can be seen that 101 condition points (808-835 s, 1044-1116 s) are selected in the high-speed phase, and the condition points are input into the control system for the bench test.

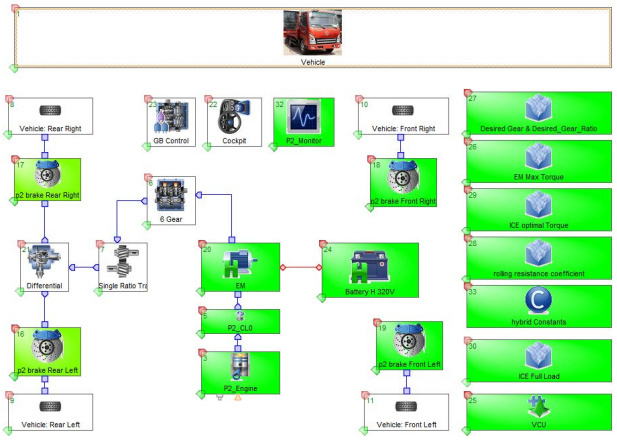

FIGURE 4. Physical model of the parallel HEV.

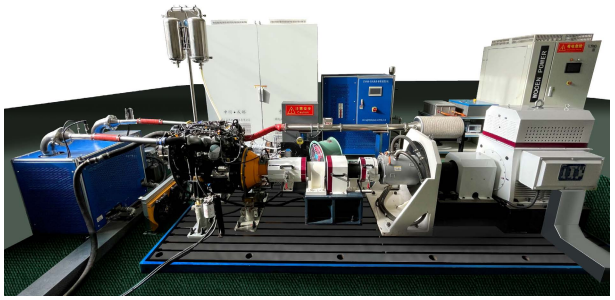

FIGURE 5. Schematic diagram of the experimental test bench for a single-axis parallel hybrid power system.

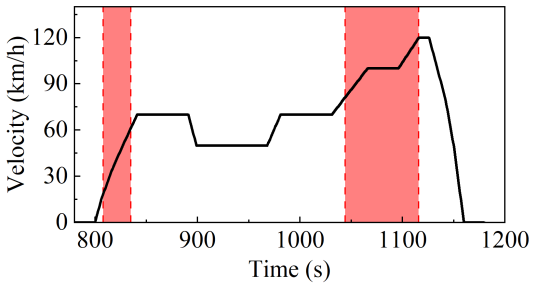

FIGURE 6. Test working point.

Fig. 7 shows the variation curves of fuel consumption of the hybrid power system under 101 operating points. From Fig. 7, it can be seen that the simulation results match well with the test result curves, proving the model's credibility.

III. ENERGY MANAGEMENT STRATEGIES

A. LOGIC-BASED ENERGY MANAGEMENT STRATEGY

The HEV adopts a logic-based torque distribution control strategy, with engine and EM torque as the direct control objects, and adopts the best torque distribution based on ensuring the performance of the whole vehicle. The control strategy working modes in this paper can be divided into

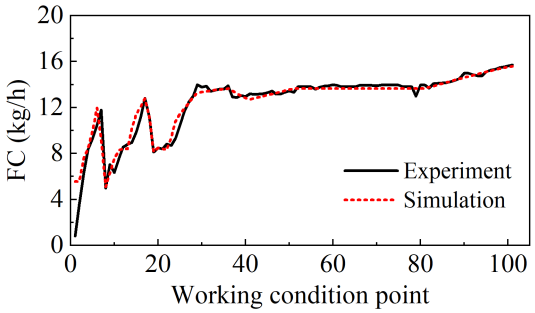

FIGURE 7. Fuel consumption change curve.

EM drive mode, drive charging mode, hybrid drive mode, regenerative braking mode, and parking mode.

When $SOC \geq SOC_{low}$, $T \geq T_{low}$, $0 \leq T_{req} \leq T_1$ or when $SOC \geq SOC_{low}$, $T_{req} \leq T_{\text{mmax}}$, $0 \leq V \leq V_1$, it enters EM drive mode.

When $V \geq V_1$, $T_1 \leq T_{req} \leq T_2$, or when $SOC < SOC_{low}$, it enters the travel charging mode.

When $SOC \geq SOC_{low}$, $V \geq V_1$, $T_{req} \geq T_2$ or when $SOC \geq SOC_{low}$, $V \geq V_1$, $T_{req} \geq T_1$, it enters the hybrid drive mode.

When $P_{\text{break}} \geq 0$ and $V > 0$, enter the brake energy recovery mode.

Where T_{req}, T_{mmax}, T_{EM}, and T_{EN} are driver demand torque, EM maximum torque, EM torque, and engine torque respectively, unit is N·m; T_1 is the torque corresponding to the engine minimum fuel consumption; T_2 is the torque corresponding to the engine high-efficiency zone at a different speed; V_1 is the speed at which the gearbox shifts at 2000 r/min second gear, unit is km/h; V_2 is to ensure that the high speed in hybrid drive mode and takes the value of 100 km/h; SOC_{low} is a low battery threshold of 0.65 and SOC_{high} is a high battery threshold of 0.75.

B. EQUIVALENT CONSUMPTION MINIMIZATION STRATEGY

The basic principle of the ECMS approach is to allocate costs to electrical energy so that the use of electrical energy storage is equivalent to the use (or saving) of a certain amount of fuel. The ECMS equates electrical consumption to fuel consumption through an EF and assigns the lowest set of torque combinations to the motor and engine. The battery is seen as an auxiliary, reversible fuel tank.

The ECMS mainly includes three core issues: first, to determine the EF, the EF mainly through the Pontryagin's minimum principle, hitting the target method, and the efficiency conversion equivalence method to determine. Second, the torque distribution of the power source is optimized to minimize the equivalent fuel consumption according to the vehicle's driving condition on the road. Third, it is ensured that the initial SOC and the final SOC have convergence at the end of the driving cycle.

The transient equivalent fuel consumption is calculated by (7).

$$\dot{m}_{\text{f,eqv}} = \dot{m}_{\text{f}} + \frac{s}{Q_{\text{lhv}}} P_{\text{batt}} \tag{7}$$

where $\dot{m}_{\text{f,eqv}}$ is the engine fuel consumption rate, the unit is g/s; Q_{lhv} is the fuel lower heating value, taken as 425000 J/g.

Neglecting the loss of energy through the transmission system, the charge and discharge efficiency of the battery is calculated by (8) and (9).

$$\eta_{\text{dis\_batt}} = \frac{P_{\text{dis\_em}}}{E_{\text{dis\_batt}}} \tag{8}$$

$$\eta_{\text{charg\_batt}} = \frac{E_{\text{charg\_batt}}}{P_{\text{charg\_em}}} \tag{9}$$

where $E_{\text{dis\_batt}}$ is the output power of the battery per unit time; $P_{\text{dis\_em}}$ is the power that the EM gets from the battery; $E_{\text{charg\_batt}}$ is the power that the battery gets from the EM per unit time; $P_{\text{charg\_em}}$ is the power generated by the EM.

The EF is calculated by (10)

$$s = \begin{cases} \dfrac{1}{\bar{\eta}_{\text{eng\_chg}} \bar{\eta}_{\text{bat\_chg}}}, & P_{\text{batt}} \geq 0 \\ \dfrac{\bar{\eta}_{\text{bat\_dis}}}{\bar{\eta}_{\text{eng\_dis}}}, & P_{\text{batt}} < 0 \end{cases} \tag{10}$$

where P_{batt} is the battery charging and discharging power, when $P_{\text{batt}} \geq 0$, means battery discharging, when $P_{\text{batt}} < 0$, means battery charging, unit kw; s is the EF; $\bar{\eta}_{\text{eng\_chg}}$ is the average efficiency of the engine under line charging; $\bar{\eta}_{\text{bat\_chg}}$ is the average charging efficiency of the battery; $\bar{\eta}_{\text{eng\_dis}}$ is the average efficiency of the engine under hybrid drive; $\bar{\eta}_{\text{bat\_dis}}$ is the average efficiency of the battery when discharging.

C. ADAPTIVE EQUIVALENT CONSUMPTION MINIMIZATION STRATEGY

1) STANDARD DRIVING CYCLE SELECTION

The standard driving cycle is mainly divided into the suburban driving cycle, urban driving cycle, and high-speed driving cycle. The main characteristics of the urban driving cycle are many intersections, overcrowded roads, and low speeds. The main characteristics of the suburban driving cycle are fewer intersections, shorter idling time of power source, and often driving at low and medium speeds. The main characteristics of the high-speed driving cycle are higher speeds and fewer vehicle stops. In this paper, the urban dynamometer driving schedule (UDDS) represents the suburban driving cycle, the New York city cycle (NYCC) represents the urban driving cycle, and the highway fuel economy test (HWFET) represents the high-speed driving cycle. The standard driving cycle is shown in Fig. 8.

2) ANALYSIS OF DRIVING CYCLE CHARACTERISTIC PARAMETERS

The characteristics of the driving cycle can be directed by the parameter characteristic. In this paper, 10 characteristic parameters are selected to describe the characteristics of the driving cycle, which are maximum speed, average speed, maximum acceleration, average acceleration, maximum deceleration, average deceleration, acceleration time ratio, deceleration time ratio, uniform speed time ratio, and

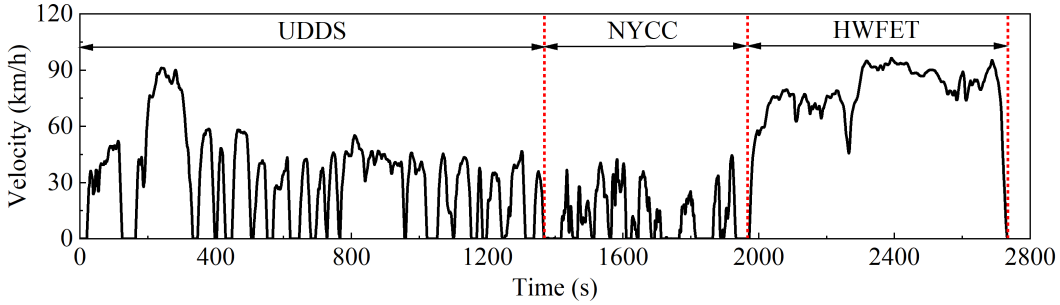

FIGURE 8. Standard driving cycle.

idling time ratio. The fixed-step analysis method is selected, and the step size of 120 s is chosen. To increase the number of micro conditions, one micro condition is taken at the midpoint of the intersection of two consecutive micro conditions.

The specific steps of the characteristic parameter solution are as follows.

(1) Load standard driving cycle data on MATLAB.

(2) Build the Simulink model, import the time and velocity series, derive the velocity, and find the acceleration at each moment.

(3) Cutting of the driving cycle using circular statements, 120 s for each micro condition.

(4) Solving for 10 characteristic parameters for each micro condition in the command window.

(5) Marking and counting for each group of micro working conditions.

3) OVERVIEW OF LEARNING VECTOR QUANTIZATION

Learning Vector Quantization (LVQ) is an output forward neural network for training output, competing and output layers, which is widely used in recognition, diagnosis, and optimization fields. If two or more input vectors are close to each other, then the competition layer will classify them into the same class. Compared with other pattern recognition, LVQ lattices are simple and do not require complex neural network structures, but only the distance between them and competing neurons.

The specific steps of the LVQ algorithm are as follows.

(1) Determine the connectivity threshold matrix between neurons and the learning efficiency.

(2) Input vector to the input neuron, according to (11) calculate the distance from the competing neuron, S1.

$$d_{\mathrm{i}} = \sqrt{\sum_{j=1}^{R} (x_{\mathrm{i}} - w_{\mathrm{ij}})^2} (i = 1, 2, .., S^1) \tag{11}$$

(3) Select the competing neuron with the smallest distance from the input vector, then the output neuron connected to it is noted as label S1.

(4) If the label S1 is the same as the input vector category, the threshold is adjusted according to (12). If the label S1 is different from the input vector category, the threshold is adjusted according to (13).

$$w_{\mathrm{ij\_new}} = w_{\mathrm{ij\_old}} + \eta(x - w_{\mathrm{ij\_old}}) \tag{12}$$

$$w_{\mathrm{ij\_new}} = w_{\mathrm{ij\_old}} - \eta(x - w_{\mathrm{ij\_old}}) \tag{13}$$

4) TRAINING LVQ-BASED DRIVING CYCLE RECOGNIZER

Based on the training samples, 80% of the data are randomly selected as the training set, and 20% of the data are used as the test set. The input neurons are set to 10, representing 10 characteristic parameters of each data set. The output neurons are set to 3, which represent the urban driving cycle, suburban driving cycle, and high-speed driving cycle. The training steps are as follows.

(1) Loading data into MATLAB and using a random function to break up the training data according to the proportional division.

(2) Calculate the proportion of different driving cycles in the training data respectively based on creating an LVQ network. LVQ network by new lvq function, and set the number of hidden layers as 10.

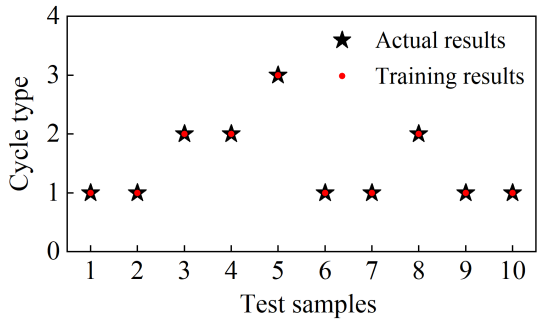

FIGURE 9. Test sample identification results.

(3) Set the grid parameters, the learning rate is 0.01, and the root means the square error is reduced to 0.1 within 1000 training iterations. The test sample recognition results are shown in Fig. 9, which shows that 20% of the test data are recognized correctly at 100%. Conducted several driving cycle recognition tests, and the results showed an average accuracy rate of 98%. Indicating that the LVQ neural network can be used for driving cycle recognition.

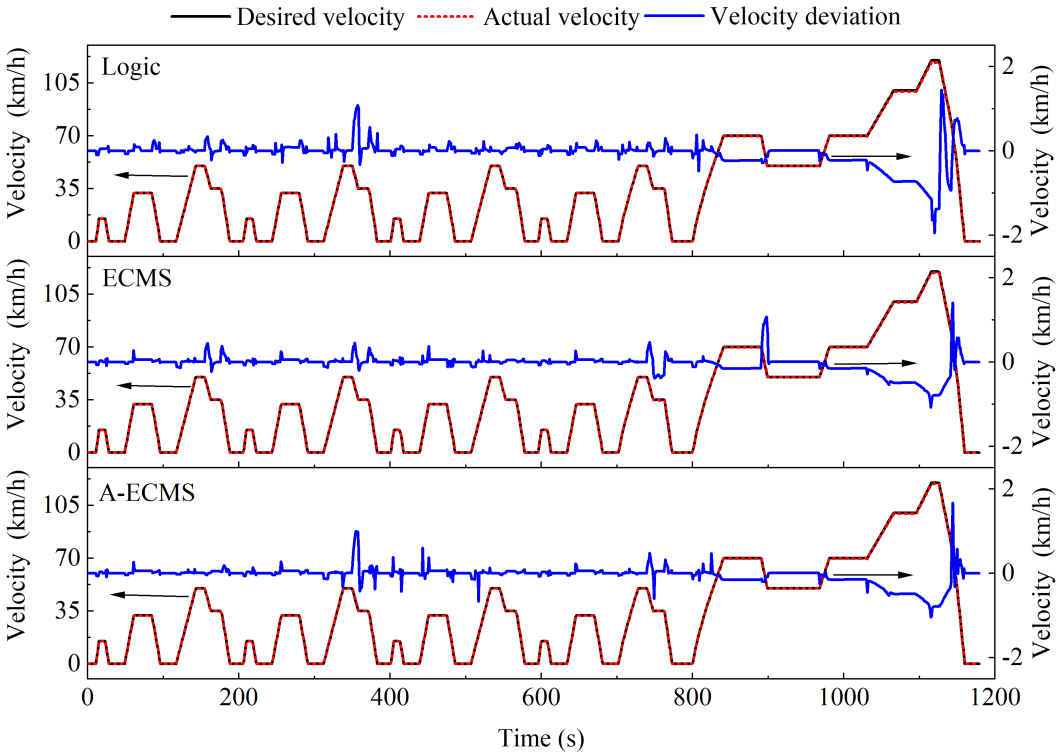

FIGURE 10. Driving cycle tracking in NEDC.

5) CONSTRUCTION OF LVQ-BASED DRIVING CYCLE RECOGNIZER

The LVQ-based driving cycle recognizer is constructed by encapsulating the LVQ neural network into a module via MATLAB/Simulink. The characteristic parameters of the driving cycle are calculated and input as vectors into the LVQ-based recognition network. The equivalent factors corresponding to the micro working conditions are represented in code and encapsulated into a Simulink module. The EF working conditions are realized offline. The internal encapsulated function is shown in (14).

$$function : (y_1, y_2, \ldots y_n) = fcn(x_1, x_2, \ldots x_n) \qquad (14)$$

where x is the function independent variable; y is the function dependent variable.

IV. SIMULATION ANALYSIS

The vehicle driving cycle is the basis for evaluating vehicle fuel economy and emission performance. Different countries have different standards. In this paper, the new European driving cycle (NEDC) and China heavy-duty commercial vehicle test cycle-truck (CHTC-LT) are selected for simulation analysis.

A. PERFORMANCE COMPARISON UNDER NEDC DRIVING CYCLE

Fig. 10 shows the speed following of different EMSs under the NEDC driving cycle. From Fig. 10, it can be seen that the actual speed of the three EMSs matches well with the target speed curve. The maximum speed error of the logic-based EMS is about 2 km/h, and the maximum speed error of both ECMS and A-ECMS is less than 2 km/h.

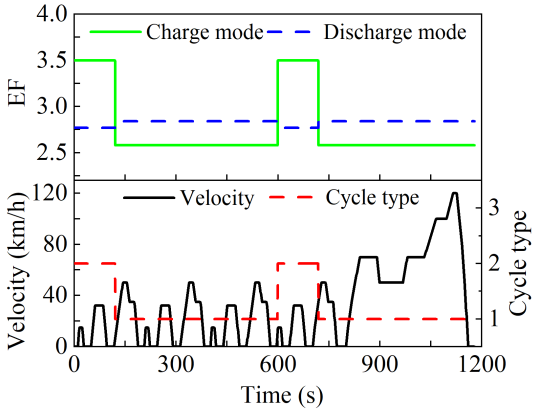

FIGURE 11. driving cycle recognition results in NEDC.

Fig. 11 shows the driving cycle recognition results in NEDC. From Fig. 11, it can be seen that the suburban driving cycle in 0-120 s and 600-720 s, and the travel charging and hybrid drive mode EF are 3.5 and 2.77, respectively. Meanwhile, the condition recognizer identifies the high-speed condition, and the travel charging and hybrid drive mode equivalence factors are 2.58 and 2.84, respectively. Recognition results in high-speed driving cycles in other

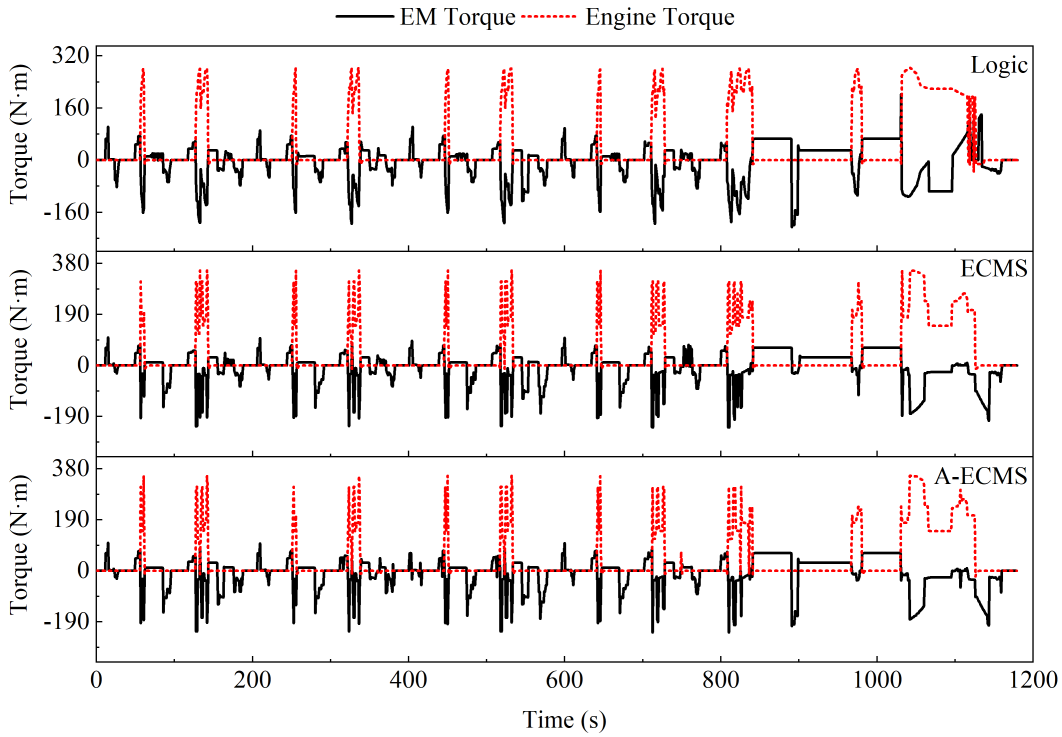

FIGURE 12. Engine and EM torque distribution in NEDC.

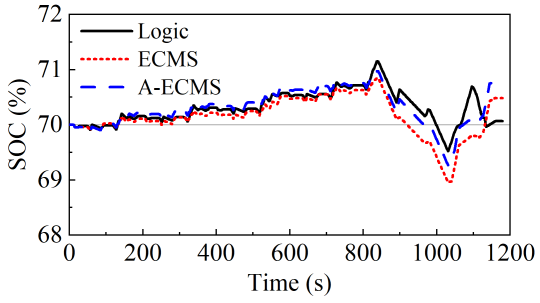

FIGURE 13. SOC variation curve in NEDC.

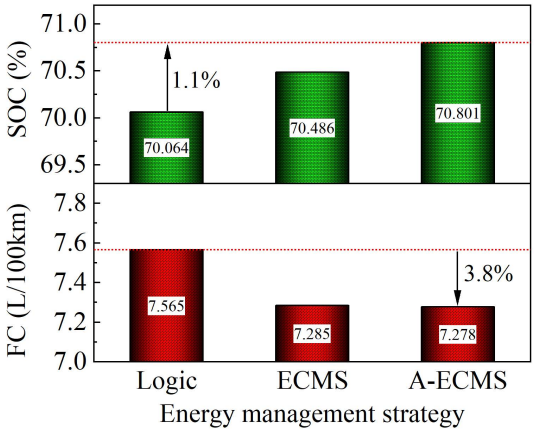

FIGURE 14. Final SOC and 100 km fuel consumption comparison in NEDC.

periods, and the charge mode and discharge mode EF are 2.58 and 2.84 respectively.

Fig. 12 shows engine and motor torque distribution in NEDC, it can be seen from Fig. 12 that the engine and motor torque change periodically during 0-780 s while the maximum engine torque is around 250 N·m. The vehicle speed increases, causing the torque to increase during 780-1180 s. Compared with the logic-based EMS, the variation of torque distribution under ECMS increases, and the number of engine starts and stops becomes more frequent. This is mainly because ECMS is solving for the minimum fuel consumption at each instant, which makes the engine turn on more frequently and the EM torque change more. Near the 1100 s, the EM torque is negative under the logic-based EMS, and the EM torque is close to 0 under the ECMS. This is because at this time the vehicle gradually shifts from the uniform speed to the acceleration state. The economy of using engine drive is better at this time based on compared fuel and electricity consumption. Compared with the ECMS, the engine torque drop is maintained near 300 N·m and the EM torque drop is maintained near 200 N·m under the A-ECMS, which adjusts the working area of the engine and EM and better optimizes the fuel economy of the vehicle.

Fig. 13 shows the SOC change curve in NEDC, that indicating under 0-780 s, the SOC is in a step-up state, and under 780-1180 s, the SOC first decreases and then increases. This is mainly because the engine and EM drive the vehicle together under the high-speed driving cycle, resulting in

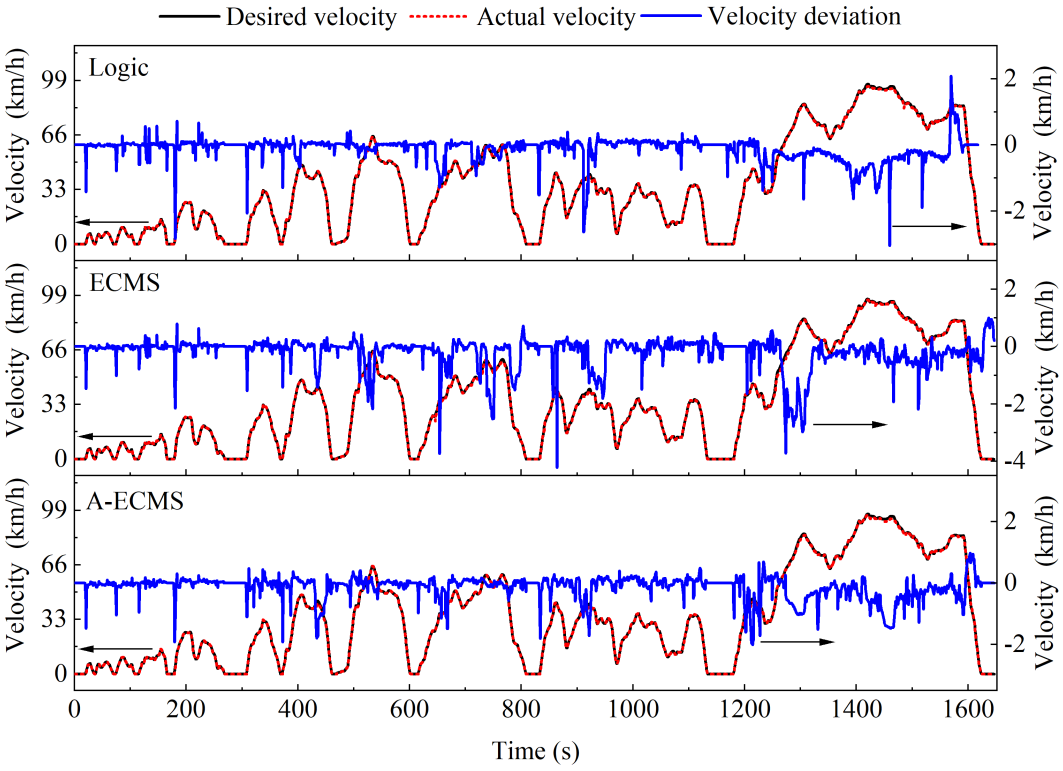

FIGURE 15. Driving cycle tracking in CHTC-LT.

the SOC is decreasing. When the vehicle speed gradually decreases, it is in regenerative braking mode, resulting in a rising SOC. The SOC changes under the three EMSs are within the range of variation.

Fig. 14 shows the comparison of final SOC and 100 km fuel consumption under the NEDC driving cycle, it can be seen from Fig. 14 that the final SOC values of the three EMSs are 70.064%, 70.486%, and 70.801%, and the 100 km fuel consumption is 7.565 L, 7.285 L, and 7.278 L, respectively. Compared with the logic-based EMS, the A-ECMS improves the final SOC by 1.1%, while reducing fuel consumption by 3.8%, indicating that A-ECMS can better improve fuel economy.

B. PERFORMANCE COMPARISON UNDER CHTC-LT DRIVING CYCLE

Fig. 15 shows the speed following of different EMSs under CHTC-LT driving cycle. From Fig. 15, it can be seen that the actual speed of the three EMSs matches well with the target speed curve, while the maximum speed error of the logic-based EMS is about 2.5 km/h. The maximum speed error of ECMS is about 4 km/h. The maximum speed error of the A-ECMS is less than 2 km/h. The A-ECMS has the best following effect.

Fig. 16 shows the driving cycle recognition results in CHTC-LT. In 0-120 s, the results of the driving cycle recognition are the urban driving cycle. The charging mode and discharge mode EF of 2.75 and 2.79, respectively. In the

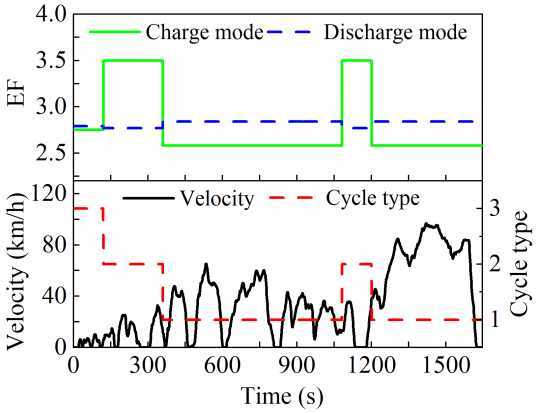

FIGURE 16. Driving cycle recognition results in CHTC-LT.

period of 120-360 s and 1080-1200 s, the results of the driving cycle recognition are the suburban driving cycle. The EF charging and discharge modes are 3.5 and 2.77, respectively. In other periods, the result of the driving cycle recognition is high-speed driving cycles. The EF charging and discharge modes are 2.58 and 2.84, respectively.

Fig. 17 shows the engine and EM torque distribution under CHTC-LT driving cycle. From Fig. 17, it can be seen that under the logic-based within 0-300 s, it is mainly driven by the EM. Under the 300-1647 s operating conditions, the maximum engine torque is nearly 250 N·m. The engine runs

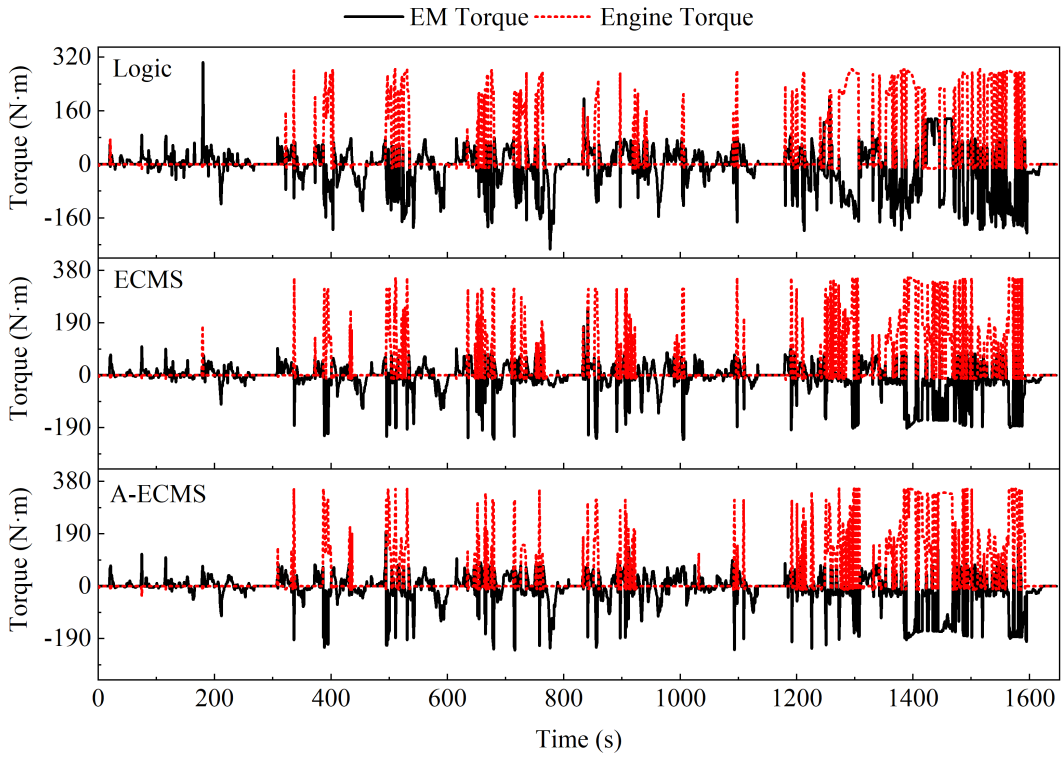

FIGURE 17. Engine and EM torque distribution in CHTC-LT.

under the economic curve, and the EM cuts the peak and fills the valley. Under ECMS in 0-300 s, it is in hybrid drive and the engine starts frequently. Under 300-1647 s operating conditions, the maximum engine torque is nearly 340 N·m, which is because the ECMS is to allocate torque by a more fuel-efficient principle at each moment, so the torque vagaries more. Around the 160 s, there is an abrupt change in the logical rule EMS motor torque due to the larger demand torque corrected by PID, which is improved under the ECMS strategy. Compared with the ECMS, under the A-ECMS, the engine torque drop is maintained near 300 N·m and the EM torque drop is maintained near 200 N·m, which better adjusts the working area of the engine and EM and optimizes the fuel economy of the vehicle.

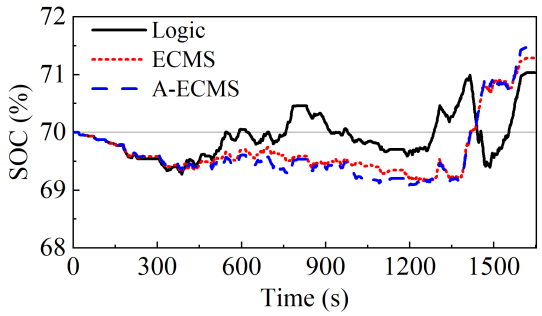

FIGURE 18. SOC variation curve in CHTC-LT.

Fig. 18 shows the SOC change curve under the CHTC-LT driving cycle. It can be seen that the SOC gradually decreases

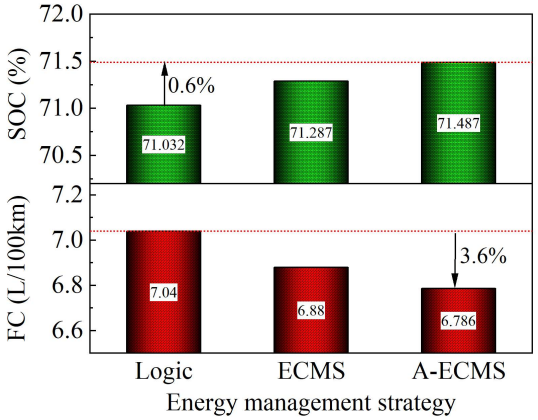

FIGURE 19. SOC and 100 km fuel consumption comparison in CHTC-LT.

from 0-300 s, which is because the vehicle mainly runs in EM driving mode at low speed. The SOC first rises and then decreases from 300-1150 s, mainly because in 0-300 s EM consumes part of the battery-electric energy, so that the vehicle runs in driving charge mode, SOC overall tends to rise. When the vehicle torque becomes large, the vehicle running in hybrid drive mode, SOC overall tends to decline. In 1150-1647 s, the vehicle running was in the driving charge mode and hybrid drive mode, so the SOC rises and then falls. When the velocity gradually drops to 0 km/h, the vehicle running in regenerative braking mode, the EM recovery part

of the energy flow to the battery, resulting in an upward trend of SOC. SOC changes under the three EMSs are within the range of change.

Fig. 19 shows the comparison of final SOC and 100 km fuel consumption under the CHTC-LT driving cycle. it can be seen from Fig. 19 that the final SOC values of the three EMSs are 71.032%, 71.28%, and 71.47%, and the 100 km fuel consumption is 7.04 L, 6.88 L, and 6.786 L, respectively. Compared with the logic-based EMS, the final SOC of the A-ECMS is improved by 0.6%, while the 100 km fuel consumption is reduced by 3.6%, indicating that A-ECMS can better improve fuel economy.

V. CONCLUSION

In this paper, we take a hybrid light truck as the target model, get the instantaneous optimal fuel consumption by the discrete engine and EM torque, establish a logic-based EMS, optimize the fuel economy, and develop the ECMS and A-ECMS. Select urban, suburban and high-speed driving cycles to obtain the characteristic parameters as a training database, and construct the LVQ-based driving cycle recognizer. The simulation results were carried out under NEDC and CHTC-LT driving cycles. Compared with the logic-based EMS, the fuel consumption of the ECMS was reduced by 3.7% and 2.27%, respectively. Compared with the ECMS, the fuel consumption of the A-ECMS was reduced by 0.96% and 1.37%, respectively, which can control the SOC variation well and achieve the expected results.

REFERENCES

[1] D.-D. Tran, M. Vafaeipour, M. El Baghdadi, R. Barrero, J. Van Mierlo, and O. Hegazy, "Thorough state-of-the-art analysis of electric and hybrid vehicle powertrains: Topologies and integrated energy management strategies," *Renew. Sustain. Energy Rev.*, vol. 119, Mar. 2020, Art. no. 109596.

[2] E. Silvas, T. Hofman, N. Murgovski, L. F. P. Etman, and M. Steinbuch, "Review of optimization strategies for system-level design in hybrid electric vehicles," *IEEE Trans. Veh. Technol.*, vol. 66, no. 1, pp. 57–70, Jan. 2017.

[3] S. Wang, X. Huang, J. M. Lopez, X. Xu, and P. Dong, "Fuzzy adaptive-equivalent consumption minimization strategy for a parallel hybrid electric vehicle," *IEEE Access*, vol. 7, pp. 133290–133303, 2019.

[4] H. Dokuyucu and M. Cakmakci, "Concurrent design of energy management and vehicle traction supervisory control algorithms for parallel hybrid electric vehicles," *IEEE Trans. Veh. Technol.*, vol. 65, no. 2, pp. 555–565, Feb. 2016.

[5] H. Banvait, S. Anwar, and Y. Chen, "A rule-based energy management strategy for plug-in hybrid electric vehicle (PHEV)," in *Proc. Amer. Control Conf.*, Jul. 2009, pp. 3938–3943.

[6] C. Wang, R. Xiong, H. He, Y. Zhang, and W. Shen, "Comparison of decomposition levels for wavelet transform based energy management in a plug-in hybrid electric vehicle," *J. Cleaner Prod.*, vol. 210, pp. 1085–1097, Feb. 2019.

[7] E. Vinot, V. Reinbold, and R. Trigui, "Global optimized design of an electric variable transmission for HEVs," *IEEE Trans. Veh. Technol.*, vol. 65, no. 8, pp. 6794–6798, Aug. 2016.

[8] J. Park, Y. L. Murphey, and M. A. Masrur, "Intelligent energy management and optimization in a hybridized all-terrain vehicle with simple on-off control of the internal combustion engine," *IEEE Trans. Veh. Technol.*, vol. 65, no. 6, pp. 4584–4596, Jun. 2016.

[9] S. Uebel, N. Murgovski, C. Tempelhahn, and B. Bäker, "Optimal energy management and velocity control of hybrid electric vehicles," *IEEE Trans. Veh. Technol.*, vol. 67, no. 1, pp. 327–337, Jan. 2018.

[10] S. Zhang, R. Xiong, and F. Sun, "Model predictive control for power management in a plug-in hybrid electric vehicle with a hybrid energy storage system," *Appl. Energy*, vol. 185, no. 1, pp. 1654–1662, Jan. 2017.

[11] Z. Chen, N. Guo, J. Shen, R. Xiao, and P. Dong, "A hierarchical energy management strategy for power-split plug-in hybrid electric vehicles considering velocity prediction," *IEEE Access*, vol. 6, pp. 33261–33274, 2018.

[12] M. Josevski and D. Abel, "Energy management of parallel hybrid electric vehicles based on stochastic model predictive control," *IFAC Proc. Volumes*, vol. 47, no. 3, pp. 2132–2137, 2014.

[13] L. Tribioli, M. Barbieri, R. Capata, E. Sciubba, E. Jannelli, and G. Bella, "A real time energy management strategy for plug-in hybrid electric vehicles based on optimal control theory," *Energy Proc.*, vol. 45, pp. 949–958, Dec. 2014.

[14] Z. Chen, C. C. Mi, B. Xia, and C. You, "Energy management of power-split plug-in hybrid electric vehicles based on simulated annealing and Pontryagin's minimum principle," *J. Power Sources*, vol. 272, pp. 160–168, Dec. 2014.

[15] H. Li, A. Ravey, A. N'Diaye, and A. Djerdir, "Equivalent consumption minimization strategy for fuel cell hybrid electric vehicle considering fuel cell degradation," in *Proc. IEEE Transp. Electrific. Conf. Expo (ITEC)*, Jun. 2017, pp. 540–544.

[16] J. Feng, Z. Han, Z. Wu, and M. Li, "A dynamic ECMS method considering vehicle speed pattern and minimum engine operation time for a range-extender electric vehicle," *IEEE Trans. Veh. Technol.*, vol. 71, no. 5, pp. 4788–4800, May 2022.

[17] X. Tian, R. He, X. Sun, Y. Cai, and Y. Xu, "An ANFIS-based ECMS for energy optimization of parallel hybrid electric bus," *IEEE Trans. Veh. Technol.*, vol. 69, no. 2, pp. 1473–1483, Feb. 2020.

[18] Y. Wang, H. Tan, Y. Wu, and J. Peng, "Hybrid electric vehicle energy management with computer vision and deep reinforcement learning," *IEEE Trans. Ind. Informat.*, vol. 17, no. 6, pp. 3857–3868, Jun. 2021.

[19] B. Hu and J. Li, "A deployment-efficient energy management strategy for connected hybrid electric vehicle based on offline reinforcement learning," *IEEE Trans. Ind. Electron.*, vol. 69, no. 9, pp. 9644–9654, Sep. 2022.

[20] S. Onori, L. Serrao, and G. Rizzoni, *Hybrid Electric Vehicles: Energy Management Strategies*. London, U.K.: Springer, 2016.

[21] Y. Wang and Z. Huang, "Optimization-based energy management strategy for a 48-V mild parallel hybrid electric power system," *J. Energy Resour. Technol.*, vol. 142, no. 5, May 2020, Art. no. 052002.

[22] L. Fan, Y. Zhang, H. Dou, and R. Zou, "Design of an integrated energy management strategy for a plug-in hybrid electric bus," *J. Power Sources*, vol. 448, Feb. 2020, Art. no. 227391.

[23] J.-C. Guan, B.-C. Chen, and Y.-Y. Wu, "Design of an adaptive power management strategy for range extended electric vehicles," *Energies*, vol. 12, no. 9, p. 1610, Apr. 2019.

[24] L. Han, X. Jiao, and Z. Zhang, "Recurrent neural network-based adaptive energy management control strategy of plug-in hybrid electric vehicles considering battery aging," *Energies*, vol. 13, no. 1, p. 202, Jan. 2020.

[25] X. Zhang and L. Zheng, "Intelligent energy control strategy for plug-in hybrid electric vehicle based on driving condition recognition," *IPPTA, Quart. J. Indian Pulp Paper Tech. Assoc.*, vol. 30, no. 5, pp. 682–692, 2018.

[26] Q. Guo, Z. Zhao, P. Shen, X. Zhan, and J. Li, "Adaptive optimal control based on driving style recognition for plug-in hybrid electric vehicle," *Energy*, vol. 186, Nov. 2019, Art. no. 115824.

[27] Q. Shi, D. Qiu, L. He, B. Wu, and Y. Li, "Support vector machine–based driving cycle recognition for dynamic equivalent fuel consumption minimization strategy with hybrid electric vehicle," *Adv. Mech. Eng.*, vol. 10, no. 11, pp. 347–349, Nov. 2018.

[28] X. Lin, K. Zhou, and H. Li, "AER adaptive control strategy via energy prediction for PHEV," *IET Intell. Transp. Syst.*, vol. 13, no. 12, pp. 1822–1831, Dec. 2019.

[29] F. Zhang, K. Xu, C. Zhou, S. Han, H. Pang, and Y. Cui, "Predictive equivalent consumption minimization strategy for hybrid electric vehicles," in *Proc. IEEE Vehicle Power Propuls. Conf. (VPPC)*, Oct. 2019, pp. 1–5.

[30] F. Zhang, J. Xi, and R. Langari, "Real-time energy management strategy based on velocity forecasts using V2V and V2I communications," *IEEE Trans. Intell. Transp. Syst.*, vol. 18, no. 2, pp. 416–430, Feb. 2017.

[31] C. Sun, F. Sun, and H. He, "Investigating adaptive-ECMS with velocity forecast ability for hybrid electric vehicles," *Appl. Energy*, vol. 185, pp. 1644–1653, Jan. 2017.

[32] X. Lin, Q. Feng, L. Mo, and H. Li, "Optimal adaptation equivalent factor of energy management strategy for plug-in CVT HEV," *Proc. Inst. Mech. Eng. D, J. Automobile Eng.*, vol. 233, no. 4, pp. 877–889, Mar. 2019.

[33] H. Li, Y. Zhou, H. Xiong, B. Fu, and Z. Huang, "Real-time control strategy for CVT-based hybrid electric vehicles considering drivability constraints," *Appl. Sci.*, vol. 9, no. 10, p. 2074, May 2019.

DONGDONG CHEN received the B.S. degree in thermal and power engineering from the North University of China, Taiyuan, China, in 2016, and the M.S. degree in power engineering from the Taiyuan University of Technology (TYUT), Taiyuan, in 2019, where he is currently pursuing the Ph.D. degree in mechanical engineering.

His research interests include energy management strategies for hybrid electric vehicles and clean alternative fuels.

TIE WANG received the B.S. and M.S. degrees in mechanical engineering from the Taiyuan University of Technology (TYUT), Taiyuan, China, in 1979 and 1989, respectively, and the Ph.D. degree in mechanical design and automation from the Beijing Institute of Technology (BIT), Beijing, China, in 2005.

He is currently a Professor and the Director of the TYUT. He is the author of four books, more than 200 articles, and presided over many national and provincial level projects. His research interests include mechanical transmission and dynamics, modern automotive design and vehicle dynamics, digital design of mechanical products, clean fuel engines, noise and vibration control of internal combustion engines, and hybrid power systems autonomous driving technology.

TIANYOU QIAO received the B.S. degree in vehicle engineering from the Hubei University of Automotive Technology, Hubei, China, in 2019, and the M.S. degree in vehicle engineering from the Taiyuan University of Technology (TYUT), in 2022.

His research interest includes energy management strategies for hybrid electric vehicles.

TIANTIAN YANG received the B.S. degree in vehicle engineering and the Ph.D. degree in mechanical engineering from the Taiyuan University of Technology (TYUT), Taiyuan, China, in 2014 and 2019, respectively.

She is currently a Lecturer at the TYUT. Her research interests include internal combustion engine combustion and vibration, diesel engine alternative fuel, and fuel injection systems.

ZHIYONG JI received the B.S. degree in vehicle engineering from the Luoyang Institute of Science and Technology, Luoyang, China, in 2015, and the M.S. degree in vehicle engineering from the Taiyuan University of Technology (TYUT), in 2019, where he is currently pursuing the Ph.D. degree in mechanical engineering.

His research interests include vehicle dynamics, intelligent control, and autonomous driving technology.